



Contents lists available at ScienceDirect

Spectrochimica Acta Part A: Molecular and Biomolecular Spectroscopy

journal homepage: www.elsevier.com/locate/saa

Molecular structure, quantum mechanical calculation and radical scavenging activities of (*E*)-4,6-dibromo-2-[(3,5-dimethylphenylimino)methyl]-3-methoxyphenol and (*E*)-4,6-dibromo-2-[(2,6-dimethylphenylimino)methyl]-3-methoxyphenol compounds



Can Alaşalvar^{a,*}, Mustafa Serkan Soylu^b, Aytaç Güder^c, Çiğdem Albayrak^d, Gökhan Apaydın^e, Nefise Dilek^f

^a Giresun University, Technical Science Vocational High School, Department of Electric and Energy, 28100 Giresun, Turkey

^b Giresun University, Faculty of Art and Science, Department of Physics, 28100 Giresun, Turkey

^c Giresun University, Vocational High School of Health Services, Department of Medical Services and Techniques, 28100 Giresun, Turkey

^d Sinop University, Faculty of Arts and Sciences, Department of Chemistry, 57000 Sinop, Turkey

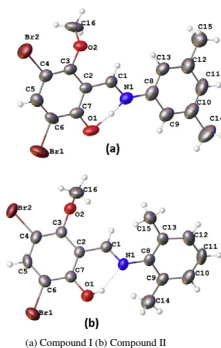
^e Karadeniz Technical University, Faculty of Arts and Sciences, Department of Physics, 61080 Trabzon, Turkey

^f Aksaray University, Faculty of Arts and Sciences, Department of Physics, 68100 Aksaray, Turkey

HIGHLIGHTS

- The title compounds were characterized using experimental and theoretical methods.
- Antioxidant properties were determined by using different methods.
- Observed and calculated values were compared.

GRAPHICAL ABSTRACT



ARTICLE INFO

Article history:

Received 30 January 2014

Received in revised form 3 March 2014

Accepted 21 March 2014

Available online 13 April 2014

Keywords:

Schiff base

Crystal structure

DFT method

Radical scavenging activities

ABSTRACT

In this study, (*E*)-4,6-dibromo-2-[(3,5-dimethylphenylimino)methyl]-3-methoxyphenol and (*E*)-4,6-dibromo-2-[(2,6-dimethylphenylimino)methyl]-3-methoxyphenol compounds have been synthesized and characterized by using X-ray crystallographic method, FT-IR and Density functional method. The molecular geometry, vibrational frequencies of the title compounds in the ground state have been calculated by using B3LYP with the 6-31G(d,p) basis set. The tautomeric form of the compounds has been demonstrated by using single crystal X-ray method, FT-IR spectrometer and DFT method. In addition, HOMO–LUMO energy gap, molecular electrostatic potential map and NBO analysis of the compounds are performed at B3LYP/6-31G(d,p) level. It may be remarked that the free radical scavenging activities of the title compounds were assessed using DPPH[•], DMPD^{•+}, and ABTS^{•+} assays. The obtained results show that especially compound 2 has effective DPPH[•] (SC_{50} 1.52 ± 0.14 µg/mL), DMPD^{•+} (SC_{50} 1.22 ± 0.21 µg/mL), and ABTS^{•+} (SC_{50} 3.32 ± 0.17 µg/mL) scavenging activities compared with standards (BHA, rutin, and trolox).

© 2014 Elsevier B.V. All rights reserved.

* Corresponding author. Tel.: +90 0454 310 14 00; fax: +90 0454 310 14 77.

E-mail address: canalasalvar@hotmail.com (C. Alaşalvar).

Introduction

Schiff bases are used as starting materials in the synthesis of important drugs such as antibiotics, antiallergics, antifungals and antitumors because of their biological activities [1,2]. On the industrial scale, they have a wide range of applications, such as in dyes and in pigments [3].

o-Hydroxy Schiff bases are of interest because they have long been known to show photochromism and thermochromism in the solid state, which can involve reversible proton transfer from an oxygen atom to the neighboring nitrogen atom. Based on thermochromic and photochromic Schiff bases, it was proposed that the molecules exhibiting thermochromism are planar while the molecules exhibiting photochromism are non-planar [4–6]. Photochromic compounds are used as optical switches and optical memories, variable electrical current, ion transport through membranes [7].

In general, Schiff bases have two possible tautomeric forms, the phenol-imine (OH) and the keto-amine (NH) forms. Depending on the tautomers, two types of intramolecular hydrogen bonds are observed in Schiff bases: O—H...N in phenol-imine [8,9] and N—H...O in keto-amine [10,11] tautomers. Another structure of Schiff base compounds is their zwitterionic form and this is rarely seen for hydroxy derivatives. The characteristic property of this form is the presence of ionic N⁺—H...O⁻ hydrogen bond [12].

In this work, we first synthesized and determined structure of the molecular of (*E*)-4,6-dibromo-2-[(3,5-dimethylphenylimino)methyl]-3-methoxyphenol (compound 1) and (*E*)-4,6-dibromo-2-[(2,6-dimethylphenylimino)methyl]-3-methoxyphenol (compound 2) compounds by using X-ray technique, FT-IR spectra and theoretical methods. Properties of investigated molecules were compared with each other. In addition, the free radical scavenging activities of the title compounds were evaluated by using a 2,2-diphenyl-1-picryl-hydrazyl (DPPH[•]), *N,N*-dimethyl-*p*-phenylenediamine (DMPD⁺), and 2,2'-azino-bis(3-ethylbenzthiazoline-6-sulfonic acid) (ABTS^{•+}) scavenging activity assays.

Experimental details

Materials and measurements

FT-IR spectra of compounds were recorded on a Perkin-Elmer spectrometer using KBr pellets. The melting points were determined by using StuartMP30 apparatus.

Synthesis

The compound (*E*)-4,6-dibromo-2-[(3,5-dimethylphenylimino)methyl]-3-methoxyphenol (1) was prepared by refluxing a mixture of a solution containing 3,5-dibromo-2-hydroxy-6-methoxybenzaldehyde (0.5 g 1.65 mmol) in 20 ml ethanol and a solution containing 3,5-dimethylaniline (0.20 g, 1.651 mmol) in 20 ml ethanol. The mixture was stirred for 2 h under reflux. The crystals of compound 1 suitable for X-ray analysis were obtained by slow evaporation from CH₃CN (yield = 83%, m.p. = 456–459 K). The same procedure was followed in synthesizing compound 2. The crystals of compound 2 were obtained from EtOH (yield = 87%, m.p. = 358–360 K).

Crystal data for the compounds

X-ray diffraction data were recorded on Bruker SMART BREEZE CCD diffractometer (purchased under Grant No. 2010K120480 of the State of Planning Organization). Absorption correction applied to collected data by multi scan, SADABS V2012/1 software [13]. The

compound 1 and 2 were solved by Direct methods [14] using SHELXS-97 and refined with SHELXL-97 [14]. The molecular figures were prepared by the help of Olex 2 program packages.

All non-hydrogen atoms were refined anisotropically. The refinement was carried out using the full matrix least squares method on the positional and anisotropic temperature parameters of non-hydrogen atoms corresponding to 194 crystallographic parameters for 1 and 193 parameters for 2. H1A atom was located in the difference maps, and their positions were refined using freely and Hydrogen atoms bonding to C atoms were refined using a riding model with fixed isotropic U values for compound 1. All H atoms were refined using a riding model with fixed isotropic U values for compound 2.

Details of the data collection conditions and the parameters of the refinement process are given in Table 1.

Determination of free radical scavenging activities

DPPH[•] radical scavenging activity assay

The DPPH radical scavenging activities of compounds and standards were evaluated according to previously method described by Blois (1958) [15] with minor modifications. Serially diluted samples (200 μL) at the different concentrations (1–10 μg/mL) was added to DPPH[•] solution (2.8 mL, 0.2 mM) in ethanol. The mixtures were shook forcefully and allowed to stand at room temperature during 30 min. Then, absorbance was recorded at 517 nm in a spectrophotometer. The results were expressed as SC₅₀ by linear regression analysis.

DMPD⁺ radical scavenging activity assay

DMPD radical scavenging activity assays were performed according to method of Fogliano et al. (1999) [16]. DMPD⁺ solutions (100 mM) was prepared by using a deionized water. This

Table 1
Crystal data, data collection and refinement detail of the title compounds.

	Compound 1	Compound 2
Empirical formula	C ₁₆ H ₁₅ Br ₂ NO ₂	C ₁₆ H ₁₅ Br ₂ NO ₂
Formula weight	413.11	413.11
Temperature/K	296(2)	296(2)
Crystal system	orthorhombic	orthorhombic
Space group	<i>Pbca</i>	<i>Pnma</i>
<i>a</i> /Å	16.987(13)	8.6731(3)
<i>b</i> /Å	<i>b</i> = 6.884(6)	15.3199(5)
<i>c</i> /Å	<i>c</i> = 27.533	24.1525(7)
α /°	90.00	90.00
β /°	90.00	90.00
γ /°	90.00	90.00
Volume/Å ³	3220(3)	3209.17(18)
<i>Z</i>	8	8
ρ_{calc} mg/mm ³	1.704	1.710
μ m ⁻¹	5.04	5.055
<i>F</i> (000)	1632	1632.0
Crystal size/mm ³	0.91 × 0.43 × 0.25	0.868 × 0.718 × 0.200
2 θ range for data collection	2.96–52°	3.38–57.02°
Index ranges	–20 ≤ <i>h</i> ≤ 20, –8 ≤ <i>k</i> ≤ 8, –33 ≤ <i>l</i> ≤ 33	–11 ≤ <i>h</i> ≤ 8, –20 ≤ <i>k</i> ≤ 20, –32 ≤ <i>l</i> ≤ 32
Reflections collected	29616	31510
Independent reflections	3161 [<i>R</i> _{int} = 0.0900, <i>R</i> _{sigma} = 0.0535]	4055 [<i>R</i> _{int} = 0.0812, <i>R</i> _{sigma} = 0.0506]
Data/restraints/parameters	3161/0/194	4055/0/194
Goodness-of-fit on <i>F</i> ²	1.181	1.191
Final <i>R</i> indexes [<i>I</i> ≥ 2 σ (<i>I</i>)]	<i>R</i> ₁ = 0.0705, <i>wR</i> ₂ = 0.2044	<i>R</i> ₁ = 0.0770, <i>wR</i> ₂ = 0.1353
Final <i>R</i> indexes [all data]	<i>R</i> ₁ = 0.1266, <i>wR</i> ₂ = 0.2429	<i>R</i> ₁ = 0.1217, <i>wR</i> ₂ = 0.1472
Largest diff. peak/hole/e Å ⁻³	0.96/–0.55	1.32/–0.44

solution (1 mL) was added to acetate buffer (100 mL, 0.1 M, pH 5.25), and the colored radical cation (DMPD^{•+}) was obtained by adding 0.2 mL of a ferric chloride solution (0.05 M) (the final concentration was 0.01 mM). This solution (225 µL) was transferred directly to the tube and absorbance values were measured at 505 nm (absorbance of control tube). Different concentrations (1–10 µg/mL) of the title compounds or standards (15 µL) and DMPD^{•+} (210 µL) were added to all tubes. After all tubes were stirred and left to stand for 10 min, a decrease in absorbance was measured at 505 nm in a spectrophotometer (absorbance of samples or standards). The buffer solution was used as a blank sample. The results were expressed as SC₅₀ by linear regression analysis using four different concentrations in triplicate and represent mean of the data.

ABTS^{•+} radical scavenging activity assay

ABTS radical cation scavenging activities of the title compounds and standards was carried out by using a chemical method described by Re et al. [17] with slight modification. For this experiment, ABTS^{•+} radical cation was generated by a reaction of 2.0 mmol/L ABTS and 2.45 mmol/L potassium persulfate. The reaction mixture was allowed to stand in the dark for 16 h at room temperature and used within 2 days. Prior to assay, the ABTS^{•+} solution was diluted with a PBS (0.1 M pH 7.4) to give an absorbance of 0.750 ± 0.020 at 734 nm in a 1 cm cuvette and equilibrated to 30 °C, the temperature at which all the assays were performed. Then, the diluted ABTS^{•+} solution (1.0 mL) was added to the title compounds or standards (3.0 mL) solution in PBS at different concentrations (1–10 µg/mL). The percentage inhibition of ABTS^{•+} was calculated for each concentration relative to a blank absorbance. The results were expressed as SC₅₀ by linear regression analysis using four different concentrations in triplicate and represent mean of the data.

Statistical analysis

Experimental results were given as mean ± S.D. of the three parallel measurements. Analysis of variance was performed by ANOVA procedures. Significant differences between means were determined by Duncan's Multiple Range tests. *P* values of <0.05 were regarded as significant and *P* values of <0.01 very significant. Both operations were done with SPSS (version 15.0.0; SPSS Inc., Chicago, IL, USA) for windows.

Computational details

All calculations were carried out with the Gauss-View molecular visualization program and Gaussian03 [18,19] program package. Starting geometries of compounds were taken from X-ray refinement data. The molecular structures of the compounds in the ground state are optimized by using B3LYP/6-31G(d,p) level. In DFT calculation, hybrid functional are also used, the Becke's three parameter functional (B3) [20] which defines the exchange functional as the linear combination of Hartree–Fock, local and gradient – corrected exchange terms. The B3 hybrid functional was used in combination with the correlation functional of Lee, Yang and Parr [21]. For the compound, vibrational frequencies were calculated by using B3LYP/6-31G(d,p) level. The Calculated frequencies were scaled by 0.9627 [22]. To investigate the reactive sites of the structure the molecular electrostatic potential was evaluated using the B3LYP/6-31G(d,p) method. In addition, the distributions and energy levels of HOMO–LUMO orbitals and NBO analysis were computed at the B3LYP/6-31G(d,p) level for the compounds.

Results and discussions

Crystallographic studies

Olex-2 [23] view of compounds is shown in Fig. 1(a and b) and crystal data, data collection and refinement details of compounds are given in Table 1. While molecule 1 is nearly planar and dihedral angles between the two rings (C2–C7 and C8–C13) in the molecule is 8.353 (6)° molecule 2 is not planar and dihedral angles between the two rings (C2–C7 and C8–C13) is 42.5389 (18)°. It is also known that Schiff bases may exhibit photochromism depending on the planarity or non-planarity, respectively [24]. Therefore, it can be said that compound 1 may exhibit thermochromism and compound 2 may exhibit photochromism. Compound 1 is stabilized by C16–H16...O¹ (Fig. 2) and C16–H16C...O¹ (Fig. 3) weak intermolecular hydrogen bond interactions (Table 2), as well as N⁺–H...O⁻ strong intramolecular interaction (Table 2). On the other hand, molecule 2 is stabilized by O–H...N intramolecular interaction (Table 2). Bond parameters of the compounds were given in Table 3. The C7–O1 (1.296 (8) Å) and C1–N1 (1.319 (7) Å) bond distances are the most important indicators for determination of the tautomeric form of compounds. While the C7–O1 bond is of a double bond for the keto-amine tautomer, this bond displays single bond character in phenol-imine tautomer. In addition, the C1–N1 bond is also a double bond in phenol-imine tautomer and of single bond length in keto-amine tautomer [25,26]. However, these bond lengths have intermediate values between single and double C–O (1.362 and 1.222 Å, respectively) and C–N (1.339 and 1.279 Å, respectively) bond distance [27]. Besides, zwitterionic forms of Schiff bases have an intramolecular ionic hydrogen bond (N⁺–H...O⁻), and their N⁺–H bond lengths are

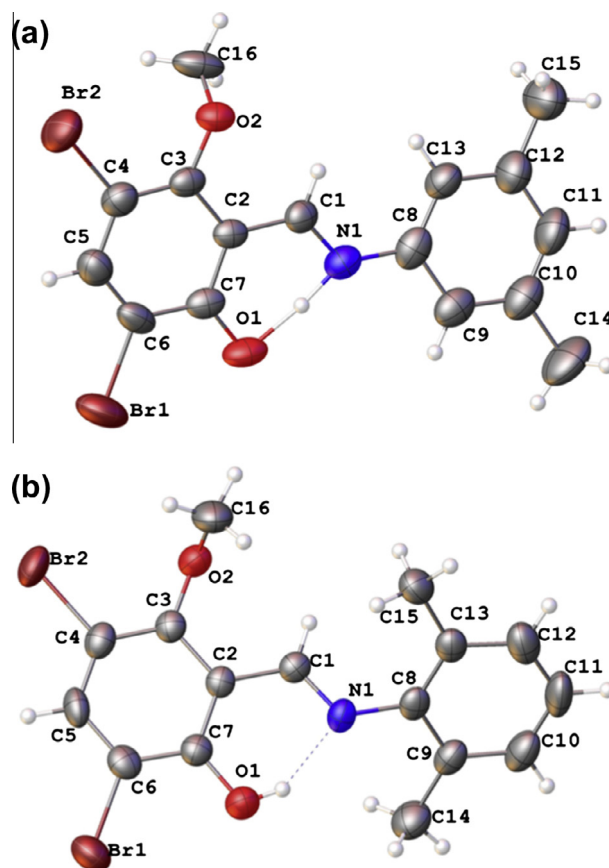


Fig. 1. (a) Olex 2 diagram of compound 1 and (b) Olex 2 diagram of compound 2.

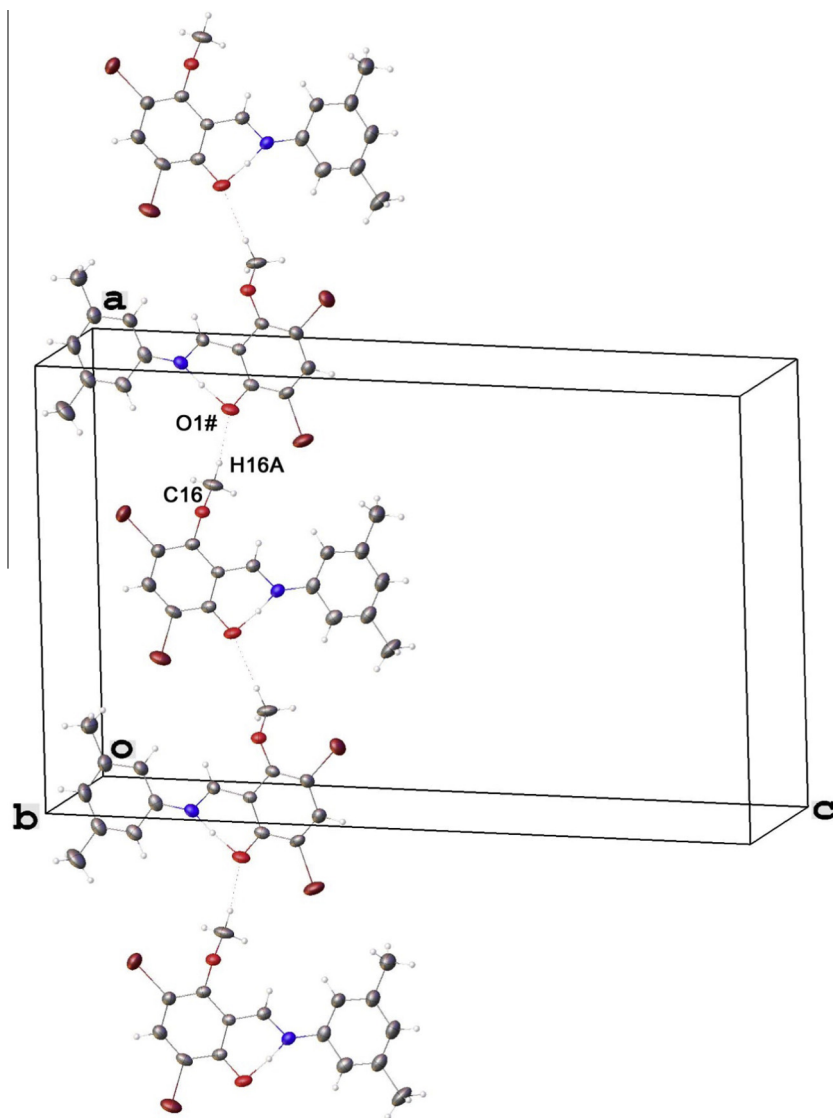


Fig. 2. C16–H16A...O1# hydrogen bond interaction of compound 1 (#:1/2 + x, y, 1/2–z).

longer than those observed in neutral N–H bond lengths (0.87 Å) [28,29]. These bond lengths are compatible with similar zwitterionic Schiff base molecules [30,31]. Considering all these, it can be said that the structure of the compound 1 has zwitterionic form. According to Table 3, C7–O1 and C1=N1 bond lengths of compound 2 were given as [1.336 (6) Å] and [1.285 (6) Å], respectively. When considering these values, C7–O1 has single bond and C1=N1 has double bond character. Hence, tautomeric form of the compound 2 is phenol-imine form. These bond distances are compatible with similar Schiff base molecules [32–38].

Optimized geometry

Optimized geometry parameters of the compounds were given together with experimental values in Table 3. As seen from Table 4, there are deviations between the calculated and experimental values for C7–O1 and C1–N1 bond distances in compound 1 but there is a good agreement between the calculated and experimental values for the compound 2. These bonds are the bonds most affected by charge transfer. Therefore, these deviations are normal. The C7–O1 and C1–N1 bond lengths of compound 1 and 2 are found to be 1.319 (7) 1.296 (8) Å and 1.336 (6), 1.285 (8) Å and

these bond lengths are calculated as 1.258, 1326 Å and 1.330, 1.289 Å for B3LYP method, respectively. C–Br bond lengths are observed between 1.880 and 1.895 Å for the molecules and these bonds are computed at the interval 1.900–1.906 Å for the B3LYP.

The compounds were optimized for both tautomeric forms using B3LYP/6-31G(d,p). According to these results, O–H form for compound 1 is more stable than N–H form and energy different between two states is 1.687 kcal/mol. This result is not compatible with the results of X-ray. Because of this inconsistency, it can be C16–H16...Oⁱ1 and C16–H16C...Oⁱ1 intermolecular interactions given in Table 2. It is well known that the experimental results belong to solid phase of molecules while the theoretical results are related to the gas phase of the isolated molecules. On the other hand, O–H form for compound 2 is more stable than N–H form and energy different between two states is 2.064 kcal/mol and this supports the results of X-ray.

FT-IR spectra analyses

FT-IR spectra of the compounds were shown in Fig. 4(a and b). Vibrational frequencies of the compounds were calculated by using

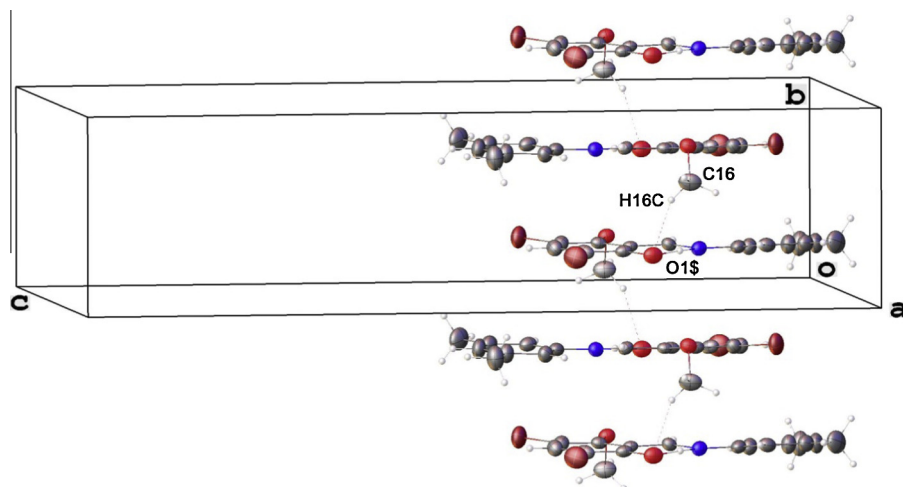


Fig. 3. C16–H16C...O1\$ hydrogen bond interaction of compound 1 (\$:1-x, -1/2+y, 1/2-z\$).

Table 2

Hydrogen-bond geometry (Å, °) of the compounds.

Compound 1				
D–H...A	D–H (Å)	H...A (Å)	D...A (Å)	D–H...A (°)
C16–H16A...O ⁱ 1	0.96	2.38	3.336 (7)	176
C16–H16C...O ⁱⁱ 1	0.96	2.51	3.394 (9)	152
N1–H1A...O1	1.13 (14)	1.39 (14)	2.522 (8)	174 (10)
Compound 2				
D–H...A	D–H (Å)	H...A (Å)	D...A (Å)	D–H...A (°)
O1–H1A...N1	0.82	1.82	2.555 (6)	148

(i) $1/2+x, y, 1/2-z$, (ii) $1-x, -1/2+y, 1/2-z$.

DFT with 6-31G(d,p) basis set and were listed in Table 4, with their experimental values.

The O–CH₃ stretching vibration bands of methoxy group for compound 1 and 2 are observed at 1047 and 1053 cm⁻¹, and these values are found at 1058 and 1061 cm⁻¹ in our B3LYP/6-31G(d,p) calculations, respectively. The obtained results are in a good agreement with literature [39–41].

According to Fig. 4a, the N–H vibration mode was observed as 3414 cm⁻¹ and this mode were calculated as 2911 cm⁻¹. The stretching frequency (N–H) observed at 3414 cm⁻¹ in compound 1 shows the presence of N–H...O intramolecular hydrogen bond given in Table 2. In the literature, some N–H modes observed for the zwitterionic Schiff bases molecules are 3191–3371 cm⁻¹ [42], 3420 cm⁻¹ [43]. The C–N, C=C and C–O vibration modes were observed as 1615, 1586 and 1311 cm⁻¹, while these modes are computed as 1628, 1583 and 1606 cm⁻¹ for B3LYP method. The N–H, C–O and C–N stretching values in the structure are compatible with similar zwitterionic Schiff base molecules [42,43].

According to Fig. 4b, the O–H vibration mode was observed as 3414 cm⁻¹ and this mode were computed as 2858 cm⁻¹. The stretching frequency (O–H) observed at 3414 cm⁻¹ in compound 1 shows the presence of O–H...N intramolecular hydrogen bond given in Table 2. In the literature, some O–H modes observed for the phenol imine Schiff bases molecules are 3414 cm⁻¹ [44], 3401 cm⁻¹ [5]. The C–N, C=C and C–O vibration modes were found as 1612, 1590 and 1337 cm⁻¹ respectively and these modes were calculated as 1618, 1579 and 1421 cm⁻¹ for B3LYP. The O–H, C–O and C–N stretching values in the structure are compatible with those of similar phenol imine Schiff base molecules [44,45].

Consequently, FT-IR results showed that compound 1 is zwitterionic form and compound 2 is phenol imine form and this support X-ray results.

Table 3

Selected molecular structure parameters of the title compounds.

Compound 1		
Bond length	X-ray (Å)	(Å)
C1–C2	1.428 (9)	1.403
C1–N1	1.296 (8)	1.326
C7–O1	1.319 (7)	1.258
C8–N1	1.419 (9)	1.408
C12–C15	1.517 (11)	1.510
C10–C14	1.508 (10)	1.510
O2–C16	1.431 (8)	1.436
C4–Br2	1.882 (7)	1.906
C6–Br1	1.887 (6)	1.900
N1–H1A	1.13 (14)	
O1–H1A	1.39 (14)	
Bond and dihedral angles	X-ray (°)	(°)
C2–C1–N1	121.8 (6)	122.30
C1–N1–C8	124.4 (6)	128.25
N1–C8–C13	123.8 (7)	123
N1–C8–C9	116.1 (7)	116.9
C1–C2–C3	119.7 (6)	119
C2–C7–O1	121.4 (6)	122
C2–C1–N1–C8	180.0 (5)	–179.51
C1–C2–C3–O2	–2.0 (8)	0.39
C1–C2–C7–O1	–3.1 (8)	–1.77
C1–N1–C8–C13	–10.7 (10)	–8.54
Compound 2		
Bond length	X-ray (Å)	(Å)
C1–C2	1.451 (7)	1.455
C1–N1	1.285 (6)	1.289
C7–O1	1.336 (6)	1.330
C8–N1	1.417 (6)	1.418
C13–C15	1.508 (8)	1.512
C9–C14	1.504 (8)	1.508
O2–C16	1.430 (7)	1.436
C4–Br2	1.895 (5)	1.905
C6–Br1	1.880 (6)	1.900
Bond and dihedral angles	X-ray (°)	(°)
C2–C1–N1	120.6 (5)	121.43
C1–N1–C8	121.9 (4)	121.35
N1–C8–C13	123.1 (5)	121.54
N1–C8–C9	115.5 (5)	117
C1–C2–C3	119.0 (4)	119.67
C2–C7–O1	120.7 (5)	121.67
C2–C3–O2	118.6 (4)	118.46
C2–C1–N1–C8	178.2 (4)	–179.56
C1–C2–C3–O2	0.0 (7)	0.68
C1–C2–C7–O1	2.4 (7)	1.41
C2–C1–N1–C8	178.2 (4)	–179.56

Table 4

Some experimental and calculated vibrational frequencies (cm^{-1}) and assignments of the compounds on B3LYP/6-31G(d,p).

Assignments	Experimental (cm^{-1})	B3LYP/6-31G(d,p) (cm^{-1})
$\nu(\text{N-H})$	3414	2911
$\nu_{\text{aromatik}}(\text{C-H})_s$	3013	3057
$\nu(\text{C-H}_3)_{\text{as}}$	2920	2999
$\nu(\text{C-H}_3)_s$	2852	2918
$\nu(\text{C-N})$	1615	1628
$\nu(\text{C=C})$	1586	1583
$\nu(\text{C=O})$	1311	1606
$\nu(\text{O-CH}_3)$	1047	1058
Compound 2		
Assignments	Experimental (cm^{-1})	B3LYP/6-31G(d,p) (cm^{-1})
$\nu(\text{O-H})_s$	3420	2858
$\nu_{\text{aromatik}}(\text{C-H})_s$	2998	3083
$\nu(\text{C-H}_3)_{\text{as}}$	2923	3014
$\nu(\text{C-H}_3)_s$	2852	2917
$\nu(\text{C=N})$	1612	1618
$\nu(\text{C=C})$	1590	1579
$\nu(\text{C=O})$	1337	1421
$\nu(\text{O-CH}_3)$	1053	1061

Molecular electrostatic potential analysis

The molecular electrostatic potential (MEP), $V(r)$ at a given point $r(x, y, z)$ in the vicinity of a molecule, is defined in terms of the interaction energy between an electrical charge which is

generated from the molecule electrons and nuclei and a positive test charge (a proton) located at r . For the studied system, the $V(r)$ values are calculated by the equation [46],

$$V(r) = \sum \frac{Z_A}{|R_A - r|} - \int \frac{\rho(r')}{|r' - r|d^3r'}$$

where Z_A is the charge of nucleus A located at R_A , $\rho(r')$ is the electronic density function of the molecule, and r' is the dummy integration variable. To predict the reactive sites of electrophilic and nucleophilic attack for the investigated compounds, the MEP at the B3LYP/6-31G(d,p) optimized geometry was calculated and shown in Fig. 5(a and b).

As seen from Fig. 5a, the most negative region is located on the O1 atom which can be considered as possible site for electrophilic attack and its $V(r)$ value is -0.054 a.u. According to Table 2, O1 atom is acceptor atom at inter and intramolecular interactions in the molecule. Therefore, MEP map supports existence of inter and intramolecular interactions given in Table 2 for the compound 1. However, the maximum positive region is located on the H atom bonded C13 and $V(r)$ value is 0.034 a.u. and this indicates a possible site for nucleophilic attack.

As seen from Fig. 5b, the most negative region are located on the O1 atom which can be considered as possible site for electrophilic attack and its $V(r)$ value is -0.043 a.u. MEP map supports existence of intramolecular interaction given in Table 2 for the compound 2. However, the maximum positive region is located on the methyl

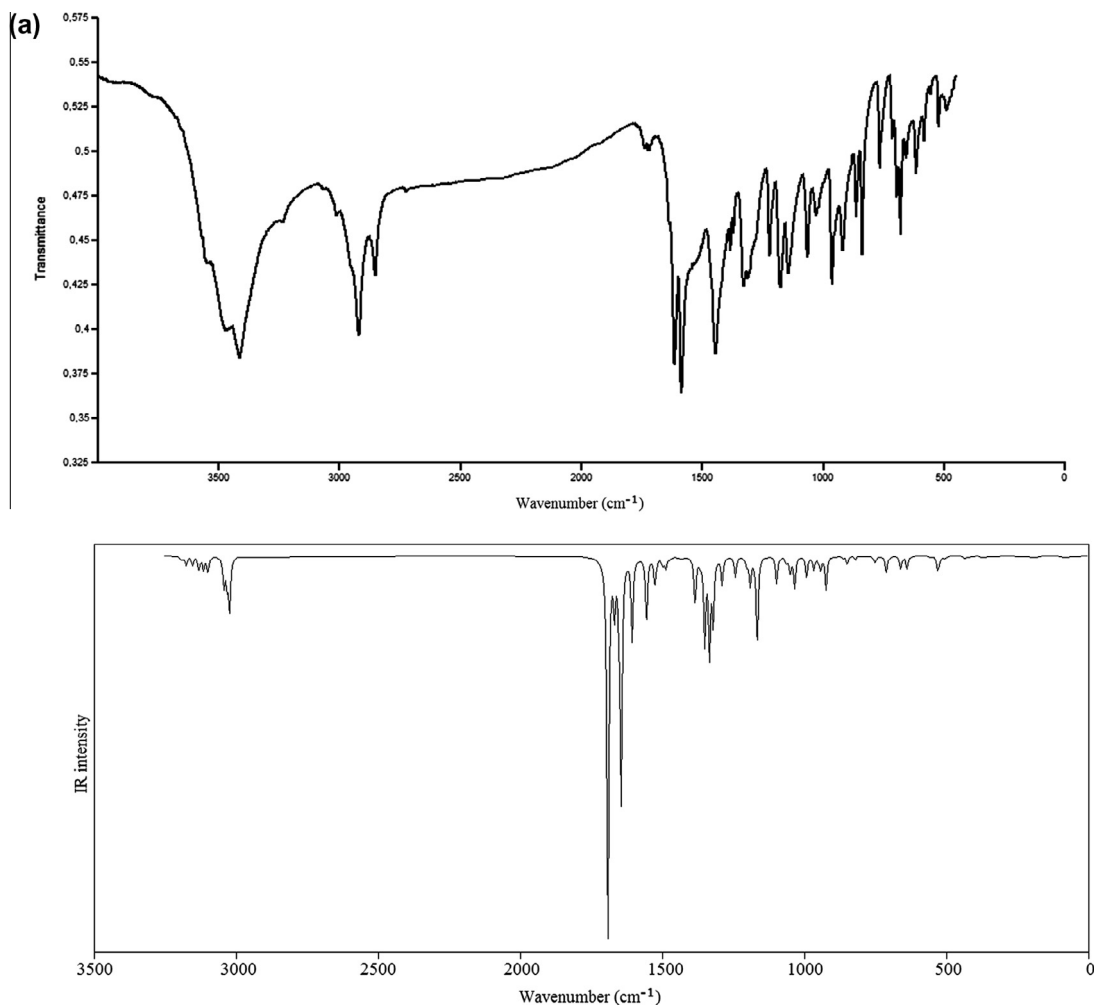


Fig. 4. (a) Experimental and calculated FT-IR spectrum of compound 1 and (b) experimental and calculated FT-IR spectrum of compound 2.

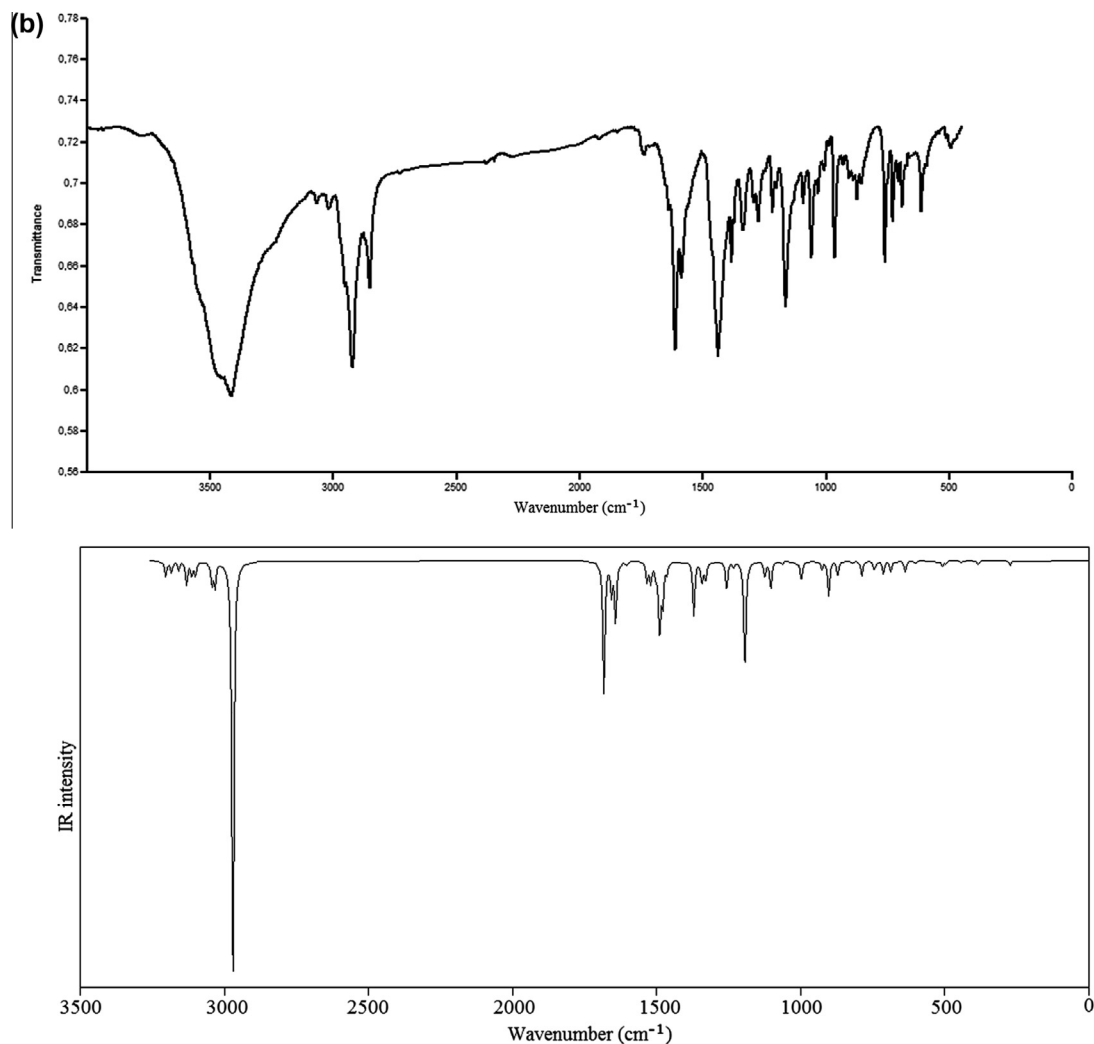


Fig. 4 (continued)

groups bonded O2 atom and $V(r)$ value is 0.024 a.u. and this indicates a possible site for nucleophilic attack.

HOMO–LUMO analysis

The most important orbitals in a molecule are the frontier molecular orbitals, called HOMO and LUMO. These orbitals determine the way the molecule interacts with other species. The frontier orbital gap helps characterize the chemical reactivity and kinetic stability of the molecule. A molecule with a small frontier orbital gap is more polarizable and is generally associated with a high chemical reactivity, low kinetic stability and is also termed as soft molecule [47,48]. The energy gap between HOMO and LUMO is a critical parameter to determine molecular electrical transport properties. By using HOMO and LUMO energy values for a molecule, chemical hardness–softness, electronegativity and electrophilicity index can be calculated as follows:

$$\mu \approx -\chi = -\frac{I+A}{2} \quad (\text{Electronegativity})$$

$$\eta \approx \frac{I-A}{2} \quad (\text{Chemical hardness})$$

$$\zeta = \frac{1}{2\eta} \quad (\text{Softness})$$

$$\psi = \frac{\mu^2}{2\eta} \quad (\text{Electrophilicity index})$$

where I and A is ionization potential and electron affinity, and is $I = -E_{\text{HOMO}}$ and $A = -E_{\text{LUMO}}$, respectively [49–52].

HOMO–LUMO orbitals of the compounds were calculated by using B3LYP/6-31G(d,p) method in gas phase. HOMO–LUMO energy gap, electronegativity, electrophilicity index and chemical hardness and softness values of the structures were listed in Table 5. 3D plots of highest occupied molecular orbitals (HOMO), lowest unoccupied molecular orbitals (LUMO) for the molecule were shown in Fig. 6(a and b). HOMO–LUMO energy gaps of the molecules are calculated as 3.11 eV and 4.08 eV respectively. According to Table 5, compound 2 has a good stability and a high chemical hardness.

NBO analysis

In order to investigate the intramolecular interactions, the bond–antibond stabilization energies within the title compounds are calculated in the NBO formalism by using second-order perturbation theory. The results of second-order perturbation theory analysis of the Fock Matrix at B3LYP/6-31G(d,p) level of theory are presented in Table 5. For each donor NBO(i) and acceptor NBO(j), the stabilization energy $E(2)$ associated with electron delocalization between donor and acceptor is estimated as [53,54]

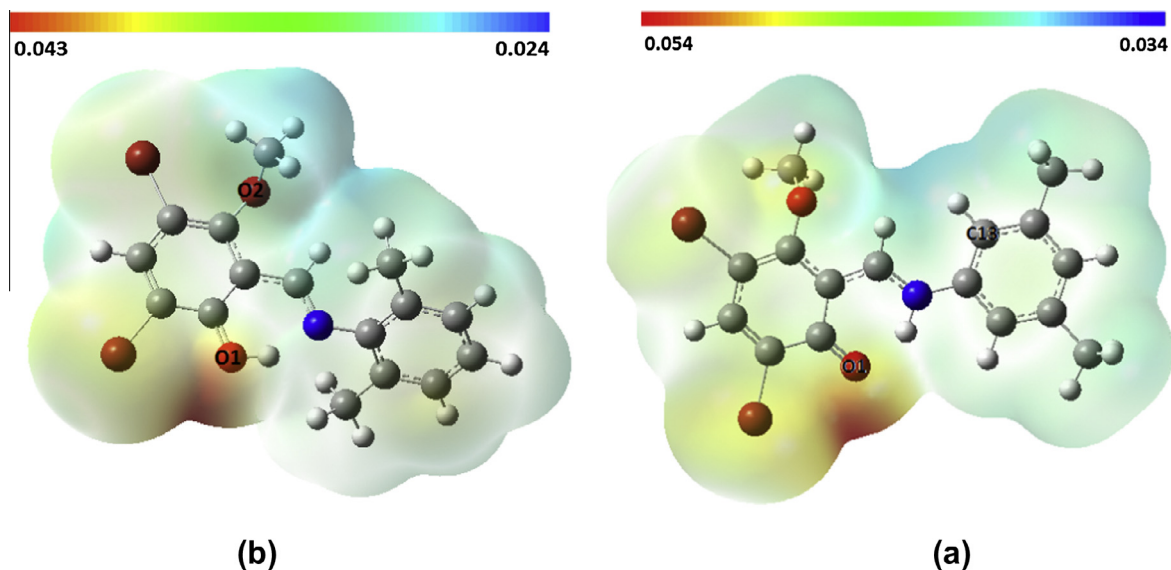


Fig. 5. (a) Molecular electrostatic potential map of compound 1 and (b) molecular electrostatic potential map of compound 2.

Table 5

The calculated HOMO, LUMO energy values, HOMO–LUMO energy gap, electrophilicity index, electronegativity, chemical hardness and softness of the molecules.

Parameters (eV)	Compound 1	Compound 2
HOMO	−5.44	6.04
LUMO	−2.32	1.96
$E_{\text{HOMO}} - E_{\text{LUMO}}$	3.11	4.08
χ (Electronegativity)	3.88	4
η (Hardness)	1.56	2.04
ζ (Softness)	0.320	0.245
ψ (Electrophilicity index)	4.82	3.92

$$E^{(2)} = -q_i \frac{(F_{ij})^2}{\varepsilon_j - \varepsilon_i} \quad (1)$$

where q_i is the donor orbital occupancy, ε_i , ε_j are diagonal elements (orbital energies) and F_{ij} is the off-diagonal NBO Fock matrix element.

In NBO analysis, the strongest stabilization in compound 1 is found in N31–H36...O32. This value is calculated as 33.76 kcal/mol in gas phase of the compound 1 and its calculated values are given in Table 6. This interactions in NBO analysis is appeared from lone pair electrons of O32 atom to antibonding sigma electrons of N31–H36 bonding, that is, it is the form $n(\text{O32}) \rightarrow \sigma^*(\text{N31} - \text{H36})$.

Therefore, we can say that these results are compatible with the obtained intra- molecular interactions from X-ray results of compound 1. Similarly, NBO analysis is also performed for compound II. But, in NBO analysis of compound II could not calculated between $n(\text{N19}) \rightarrow \sigma^*(\text{O18} - \text{H26})$ interactions because as seen in Table 2, O1–H1A...N1 intramolecular interaction of compound II is very week.

Radical scavenging activity

Antioxidant properties, especially radical-scavenging activities, are very important due to the deleterious role of free radicals in foods and in biological systems. Excessive formation of free radicals accelerates the oxidation of lipids in foods and decreases food quality and consumer acceptance [55]. The involvement of free radicals, especially their increased production, appears to be a feature of most, if not all, human diseases, including cardiovascular disease and cancer [56]. In DPPH radical form absorbs at 517 nm. When a hydrogen atom or electron was transferred to the odd electron in DPPH, the absorbance at 517 nm decreased proportionally to the increases of nonradical forms of DPPH [57,58]. As a consequence, DPPH \cdot is usually used as a substrate to evaluate the antioxidative activity of antioxidants [59]. In the manner of Table 7, the SC₅₀ values ($\mu\text{g}/\text{mL}$) of the title compounds and standards on the

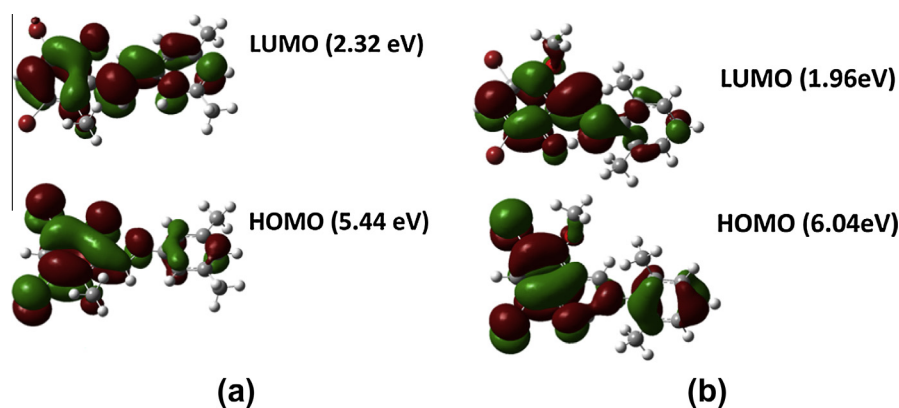


Fig. 6. (a) 3D plots of the HOMO–LUMO of the compound 1 and (b) 3D plots of the HOMO–LUMO of the compound 2.

Table 6

Second-order perturbation theory analysis of the Fock matrix in NBO basis, calculated at B3LYP/6-31G(d,p) level.

ED (e) (i)	Donor (i)	ED (e) (j)	Acceptor (j)	$E^{(2)}$ kcal mol	$E_{(j)} - E_{(i)}$ a.u.	$F_{(ij)}$ a.u.
1.80023	n(O32)	0.08383	σ^* (N31–H36)	6.75	1.06	0.076
1.85489	n(O32)	0.08383	σ^* (N31–H36)	27.01	0.71	0.125

Table 7Comparison of the DPPH \cdot , ABTS $^{+}$, and DMPD $^{+}$ radical scavenging activities of title compound and standards. BHA (butylated hydroxyanisole), RUT: rutin, TRO: trolox.

SC ₅₀ (μ g/mL)	Compound 1	Compound 2	BHA	RUT	TRO
DPPH \cdot	2.14 \pm 0.27	1.52 \pm 0.14	8.67 \pm 0.13	17.60 \pm 0.19	26.47 \pm 0.16
DMPD $^{+}$	2.08 \pm 0.07	1.22 \pm 0.21	14.41 \pm 0.19	10.99 \pm 0.03	27.84 \pm 0.27
ABTS $^{+}$	4.49 \pm 0.06	3.32 \pm 0.17	8.01 \pm 0.22	17.02 \pm 0.03	4.28 \pm 0.10

DPPH \cdot increased in that order: Compound 2 (1.52 \pm 0.14) > Compound 1 (2.14 \pm 0.27) > BHA (8.67 \pm 0.13) > Rutin (17.60 \pm 0.19) > Trolox (26.47 \pm 0.16) ($P < 0.05$).

The samples were analyzed for the ability to scavenge the DMPD radicals. The discoloration of the DMPD $^{+}$ solution was found to increase with an increase in the concentration of the sample [60]. The title compounds were an effective DMPD $^{+}$ radical scavenger in a concentration-dependent manner (1–10 μ g/mL). SC₅₀ value for the title compounds were 2.08 \pm 0.07 and 1.22 \pm 0.21 μ g/mL, respectively (Table 7). These values were found as 10.99 \pm 0.03, 14.41 \pm 0.19, and 27.84 \pm 0.27 μ g/mL for rutin, BHA, and trolox, respectively ($P < 0.01$).

ABTS $^{+}$, a protonated radical, has a characteristic maximum absorbance peak at 734 nm, which decreases with the scavenging of the proton radicals. The ABTS $^{+}$ radical cation can be prepared employing different oxidants. Results obtained using potassium persulfate as oxidant show that the presence of peroxodisulfate increases the rate of ABTS $^{+}$ auto-bleaching in a concentration-dependent manner. ABTS $^{+}$ radical cation was generated in the ABTS/K₂S₂O₈ system [61]. For radical scavenging activities, the SC₅₀ values of the title compounds and standards are reported in Table 7. The results show that ABTS $^{+}$ radical cation scavenging activity of the title compound is very important as well as standards such as BHA and rutin. SC₅₀ values (μ g/mL) of the title compounds and standards on the ABTS $^{+}$ radical cation decreased in that order: Compound 2 (3.32 \pm 0.17) < Trolox (4.28 \pm 0.10) < Compound 1 (4.49 \pm 0.06) < BHA (8.01 \pm 0.22) < Rutin (17.02 \pm 0.03) ($P < 0.01$).

Conclusion

(*E*)-4,6-dibromo-2-[(3,5-dimethylphenylimino)methyl]-3-methoxyphenol (1) and (*E*)-4,6-dibromo-2-[(2,6-dimethylphenylimino)methyl]-3-methoxyphenol (2) compounds have been characterized by using FT-IR and X-ray technique experimentally and using B3LYP method with 6-31G(d,p) basis set theoretically. According to X-ray results, it was founded the molecule 1 is nearly planar and zwitterionic form. Hence, it can be said the compound 1 has thermochromism properties. However, it was founded the molecule 2 is not planar and its tautomeric form is phenol-imine form. Therefore, it can be said that the compound 2 has photochromic properties. Intermolecular and intramolecular interactions of the title compounds were determined by X-ray technique. According to X-ray results, compound 1 is stabilized by C16–H16...O¹ and C16–H16C...O¹ weak intermolecular hydrogen bond interaction, as well as N⁺–H...O[–] strong intramolecular interaction and compound 2 is stabilized by O–H...N strong intramolecular interaction. Molecular geometry parameters and vibrational

frequencies values of the title compounds were calculated by using B3LYP method with 6-31G(d,p) basis set. Calculated values were founded to be compatible with experimental data. Electrophilic and nucleophilic attack sites of the title molecules were determined by using The MEP map. We have been calculated the parameters such as HOMO–LUMO energy gap, electronegativity, electrophilicity index and chemical hardness and softness values by means of HOMO–LUMO energy values for the title compounds. Compound 2 has a good stability and a high chemical hardness than compound 1. In addition, synthesized compounds have electron donating groups on the phenyl ring exhibiting good activity with maximum scavenging free radical. Compound 2 has electron donating groups at *ortho* and *para* positions of aromatic ring to which a nitrogen atom is bonded. Methyl groups located at *ortho* and *para* positions of aromatic ring have an important role in the stabilization of radical occurring in phenol ring. For Compound 1, the methyl groups are not effective in stabilizing phenol radical. Therefore, the effect of Compound 2 is greater than Compound 1. For this reason, this compound may be used in molecular design of free-radical-scavenging drugs in pharmaceutical and medical industry.

Supplementary material

Crystallographic data for the structures reported in this article have been deposited with the Cambridge Crystallographic Data Centre as supplementary publication number 978729 (compound I) – 978730 (compound II). Copies of the data can be obtained free of charge on application to CCDC 12 Union Road, Cambridge CB21 3EZ, UK. Fax: +44 1223 336 033; e-mail: data_request@ccdc.cam.ac.uk.

Acknowledgment

The authors acknowledge the Aksaray University Science and Technology Application and Research Center, Aksaray, Turkey, for use of the Bruker SMART BREEZE CCD diffractometer (purchased under grant No. 2010K120480 of the State of Planning Organization). The synthesis of the compounds in this study was financially supported by Sinop University in Turkey (Project No. EGTf-1901-12-03).

References

- [1] R.H. Lozier, R.A. Bogomolni, W. Stoeckenius, *Biophys. J.* 15 (1975) 955–962.
- [2] E.M. Hodnett, W.J. Dunn, *J. Med. Chem.* 13 (1970) 768–770.
- [3] A.E. Taggi, A.M. Hafez, H. Wack, B. Young, D. Ferraris, T. Lectka, *J. Am. Chem. Soc.* 124 (2002) 6626–6635.
- [4] M.D. Cohen, G.M.J. Schmidt, S. Flavian, *J. Chem. Soc.* 2041 (1964).
- [5] I. Moustakali, I. Mavridis, E. Hadjoudis, *Acta Cryst. A* 46 (1978) 467.
- [6] E. Hadjoudis, M. Vitterakis, I. Moustakali, I. Mavridis, *Tetrahedron* 43 (1987) 1345.
- [7] H. Dürr, H. Bouas-Laurent, *Photochromism: Molecules and Systems*, Elsevier, Amsterdam, 1990, pp. 685–710.
- [8] O. Sahin, O. Büyükgüngör, C. Albayrak, M. Odabaşoğlu, *Acta Crystallogr. E* 61 (2005) o1288.
- [9] A. Özek, Ç. Albayrak, M. Odabaşoğlu, O. Büyükgüngör, *Acta Crystallogr. C* 63 (2007) o177.
- [10] H. Karabiyik, N. Ocak İskeleli, H. Petek, Ç. Albayrak, E. Ağar, *J. Mol. Struct.* 873 (2008) 130.
- [11] A. Özek, S. Yuce, Ç. Albayrak, M. Odabaşoğlu, O. Büyükgüngör, *Acta Crystallogr. E* 60 (2004) o828.
- [12] A. Trzesowska-Kruszyska, *Struct. Chem.* 21 (2010) 131.

- [13] Bruker, APEX2, SAINT, SADABS and SHELXTL Bruker AXS Inc., Madison, Wisconsin, USA, 2012.
- [14] G.M. Sheldrick, SHELXS97, SHELXL97, University of Gottingen, Germany, 1997.
- [15] M.S. Blois, *Nature* 26 (1958) 1199–1200.
- [16] V. Fogliano, V. Verde, G. Randazzo, A. Ritieni, *J. Agric. Food Chem.* 47 (1999) 1035–1040.
- [17] R. Re, N. Pellegrini, A. Progettente, A. Pannala, M. Yang, C. Rice-Evans, *Free Radical Biol. Med.* 26 (1999) 1231–1237.
- [18] M.J. Frisch, G.W. Trucks, H.B. Schlegel, G.E. Scuseria, M.A. Robb, J.R. Cheeseman, J.A. Montgomery Jr., T. Vreven, K.N. Kudin, J.C. Burant, J.M. Millam, S.S. Iyengar, J. Tomasi, V. Barone, B. Mennucci, M. Cossi, G. Scalmani, N. Rega, G.A. Petersson, H. Nakatsuji, M. Hada, M. Ehara, K. Toyota, R. Fukuda, J. Hasegawa, M. Ishida, T. Nakajima, Y. Honda, O. Kitao, H. Nakai, M. Klene, X. Li, J.E. Knox, H.P. Hratchian, J.B. Cross, V. Bakken, C. Adamo, J. Jaramillo, R. Gomperts, R.E. Stratmann, O. Yazyev, A.J. Austin, R. Cammi, C. Pomelli, J.W. Ochterski, P.Y. Ayala, K. Morokuma, G.A. Voth, P. Salvador, J.J. Dannenberg, V.G. Zakrzewski, S. Dapprich, A.D. Daniels, M.C. Strain, O. Farkas, D.K. Malick, A.D. Rabuck, K. Raghavachari, J.B. Foresman, J.V. Ortiz, Q. Cui, A.G. Baboul, S. Clifford, J. Cioslowski, B.B. Stefanov, G. Liu, A. Liashenko, P. Piskorz, I. Komaromi, R.L. Martin, D.J. Fox, T. Keith, M.A. Al-Laham, C.Y. Peng, A. Nanayakkara, M. Challacombe, P.M.W. Gill, B. Johnson, W. Chen, M.W. Wong, C. Gonzalez, J.A. Pople, *Gaussian 03*, Gaussian Inc., Pittsburgh PA, 2003.
- [19] A. Frisch, L.R. Dennington, T. Keith, J. Millam, A.B. Nielsen, A.J. Holder, J. Hiscoks, Reference, Version 4.0, Gaussian Inc., Pittsburgh, 2007.
- [20] A.D. Becke, *J. Chem. Phys.* 98 (1993) 5648–5652.
- [21] C. Lee, W. Yang, R.G. Parr, *Phys. Rev. B* 37 (1988) 785–789.
- [22] A.P. Scott, L. Radom, *J. Phys. Chem.* 100 (41) (1996) 16502.
- [23] O.V. Dolomanov, L.J. Bourhis, R.J. Gildea, J.A.K. Howard, H. Puschmann, OLEX2: a complete structure solution, refinement and analysis program, *J. Appl. Cryst.* 42 (2009) 339–341.
- [24] I.M. Mavridis, E. Hadjoudis, A. Mavridis, *Acta Crystallogr. B* 34 (1978) 3709.
- [25] H. Petek, Ç. Albayrak, M. Odabaşoğlu, I. Şenel, O. Buyukgungor, *J. Chem. Cryst.* 38 (2008) 901.
- [26] C. Albayrak, B. Kosar, S. Demir, M. Odabaşoğlu, O. Buyukgungor, *J. Mol. Struct.* 963 (2010) 211.
- [27] F.H. Allen, O. Kennard, D.G. Watson, L. Brammer, A.G. Orpen, R. Taylor, *J. Chem. Soc. Perkin Trans. 2* (1987) S1.
- [28] G. Wojciechowski, M. Ratajczak-Sitarz, A. Katrusiak, W. Schilf, P. Przybylski, B. Brzezinski, *J. Mol. Struct.* 650 (2003) 191–199.
- [29] H. Petek, Ç. Albayrak, E. Ağar, H. Kalkan, *Acta Crystallogr. E* 62 (2006) 3685.
- [30] H. Petek, Ç. Albayrak, N. Ocak-İskeleli, E. Ağar, I. Şenel, *J. Chem. Cryst.* 37 (2007) 285–290.
- [31] G. Alpaslan, M. Macit, A. Erdönmez, O. Büyükgüngör, *J. Mol. Struct.* 997 (2011) 70–77.
- [32] H. Ünver, M. Yıldız, H. Özay, T. Nuri Durlu, *Spectrochim. Acta A* 74 (2009) 1095–1099.
- [33] C. Albayrak, B. Koşar, S. Demir, M. Odabaşoğlu, O. Buyukgungör, *J. Mol. Struct.* 963 (2010) 211.
- [34] Z.S. Şahin, S. Gümüş, M. Macit, I. Şamil, *Acta Crystallogr. E* 65 (2009) o3022.
- [35] G. Alpaslan, M. Macit, A. Erdönmez, O. Büyükgüngör, *J. Mol. Struct.* 1016 (2012) 22–29.
- [36] Y.B. Alpaslan, G. Alpaslan, A.A. Ağar, N.O. İskeleli, E. Öztekin, *J. Mol. Struct.* 995 (2011) 58–65.
- [37] H. Ünver, A. Karakaş, A. Elmali, T.N. Durlu, *J. Mol. Struct.* 737 (2005) 131–137.
- [38] H. Ünver, M. Yıldız, B. Dolgu, Ö. Özgen, E. Kendi, T.N. Durlu, *J. Mol. Struct.* 737 (2005) 159–164.
- [39] A. Abbas, S. Bahçeli, H. Gökçe, M. Bolte, S. Hussain, M.K. Rauf, *Spectrochim. Acta Part A* 116 (2013) 599–609.
- [40] H. Gökçe, O. Akyıldırım, S. Bahçeli, H. Yüksek, Ö.G. Kol, *J. Mol. Struct.* 1056 (2014) 273–284.
- [41] H. Gökçe, S. Bahçeli, O. Akyıldırım, H. Yüksek, Ö.G. Kol, *Lett. Org. Chem.* 10 (2013) 395–441.
- [42] G. Alpaslan, H. Tanak, A.A. Ağar, A. Erdönmez, Ş. Işık, *Struct. Chem.* 21 (2010) 1027–1036.
- [43] G. Alpaslan, M. Macit, A. Erdönmez, O. Büyükgüngör, *J. Mol. Struct.* 997 (2011) 70–77.
- [44] H. Ünver, M. Yıldız, H. Özay, T.N. Durlu, *Spectrochim. Acta Part A* 74 (2009) 1095–1099.
- [45] M. Yıldız, H. Ünver, D. Erdener, N. Ocak, A. Erdönmez, T. Nuri Durlu, *Cryst. Res. Technol.* 41 (6) (2006) 600–606.
- [46] P. Politzer, J.S. Murray, *Theor. Chem. Acc.* 108 (2002) 134–142.
- [47] L. Xiao-Hong, L. Xiang-Ru, Z. Xian-Zhou, *Spectrochim. Acta Part A* 78 (2011) 528–536.
- [48] I. Fleming, *Frontier Orbitals and Organic Chemical Reactions*, John Wiley and Sons, New York, 1976.
- [49] H. Gökçe, S. Bahçeli, *Spectrochim. Acta A* 114 (2013) 61–73.
- [50] W. Kohn, A.D. Becke, R.G. Parr, *J. Phys. Chem.* 100 (31) (1996) 12974–12980.
- [51] R.G. Parr, R.G. Pearson, *J. Am. Chem. Soc.* 105 (26) (1983) 7512–7516.
- [52] R.G. Pearson, *Proc. Natl. Acad. Sci. USA* 83 (22) (1986) 8440–8441.
- [53] D.W. Schwenke, D.G. Truhlar, *J. Chem. Phys.* 82 (1985) 2418–2427.
- [54] M. Gutowski, G. Chalasinski, *J. Chem. Phys.* 98 (1993) 4728–4738.
- [55] C.C. Akoh, D.B. Min, *Food Lipids: Chemistry, Nutrition, and Biotechnology*, Marcel Dekker, New York, 2002, pp. 283–296.
- [56] N. Deighton, R. Brennan, C. Finn, H.V. Davies, *Antioxidant properties of domesticated and wild Rubus species*, *J. Sci. Food Agric.* 80 (2000) 1307–1313.
- [57] A. Güder, H. Korkmaz, *Iran. J. Pharm. Res.* 11 (2012) 913–923.
- [58] A. Güder, M.S. Engin, M. Yolcu, M. Gür, *J. Food Process. Preserv.* (2013), <http://dx.doi.org/10.1111/jfpp.12132>.
- [59] J. Ancerewicz, E. Migliavacca, P.A. Carruport, B. Testa, F. Bree, R. Zini, J.P. Tillement, S. Labidelle, D. Guyot, A.M. Chauvet-Monges, A. Crevat, A. Le Ridant, *Free Radical Biol. Med.* 25 (1998) 113–120.
- [60] E. Koksal, E. Bursal, E. Dikici, F. Tozoglu, İ. Gulcin, *J. Med. Plant Res.* 5 (2011) 217–222.
- [61] İ. Gülçin, *Innov. Food Sci. Emerg. Technol.* 11 (2010) 210–218.